Bulletin of Environmental Contamination and Toxicology (2022) 108:379–385
https://doi.org/10.1007/s00128-021-03351-z

Ultrasensitive and Highly Selective Detection of Bisphenol a Using Core-Shell Magnetic Molecularly Imprinted Quantum Dots Electrochemiluminescent Probe

Jianjun Shi[1,2] · Xinyi Zhang[1,2] · Qianqian Zhang[1] · Ping Yang[1]

Received: 20 March 2021 / Accepted: 24 July 2021 / Published online: 11 August 2021

Abstract

The main aim of this work was to develop a magnetic molecularly imprinted polymer (MMIP)-based quantum dots electrochemiluminescent (ECL) probe for the ultrasensitive and highly selective detection of bisphenol A (BPA). The prepared core-shell Fe_3O_4@SiO_2 exhibited superparamagnetic properties, making them easy to separate. The MIP was fabricated by the self-polymerization of dopamine on the surface of amine-terminated Fe_3O_4@SiO_2 (Fe_3O_4@SiO_2-NH_2) magnetic nanoparticles and doped with quantum dots (QDs) to form an ECL system. The ECL intensity decrease with the concentration of BPA increased, due to the BPA molecules occupied molecularly imprinted sites and blocked the strong ECL emission of QDs. The prepared ECL sensor performed satisfactorily in the detection of BPA, with a wide linear range from 10^{-4} to 10^{-9} mol L^{-1} and a low detection limit of 3.4×10^{-10} mol L^{-1} (S/N = 3). The recoveries of BPA achieved were in the range 96%–107% in the detection of actual water samples. The proposed ECL sensor displayed high sensitivity and stability, and may provide an approach for determining other important analytes.

Keywords Electrochemiluminescent sensor · Quantum dots · Molecularly imprinted polymer · Magnetic core-shell nanoparticles · Bisphenol A

Endocrine-disrupting chemicals (EDCs), also known as environmental estrogens, are a class of exogenous chemicals that interfere with the biological endocrine system (Li et al. 2019). With the advance of industrialization, EDCs have received considerable public attention in recent decades. Among them, bisphenol A (2,2-bis(4-hydroxyphenyl) propane) (BPA) is one of the most ubiquitous endocrine disruptors. It is widely used in the industrial manufacture of epoxy resins and polycarbonate, and as an additive in many commercial products (Liu and Martin 2017), including baby bottles, beverage packaging, food containers, sealants, sports equipment, and medical equipment, and is therefore closely related to human daily life. BPA is mainly released into the environment in wastewater or soil from industrial landfill sites, leading to its distribution in surface water and soil ecosystems (Wang et al. 2018; Freitas et al. 2020).

Some general detection techniques have been reported for monitoring BPA, such as high-performance liquid chromatography (HPLC) (Watabe et al. 2004), gas chromatography coupled with mass spectrometry (GC-MS) (Fernandez et al. 2017), and enzyme-linked immunosorbent assays (ELISA) (Peng et al. 2016). However, compared with these methods, electrochemical sensors, having inherent advantages of low cost, fast responses with low time consumption, simple operation, convenient instrumentation, ease of miniaturization, and on-line detection, have been more widely reported (Wang et al. 2015).

Recently, more attention has been paid to the combination of magnetic nanomaterials and molecular imprinting technology. Magnetic nanoparticles can be easily separated from a reaction medium without centrifugation by using an external magnetic field (Liu et al. 2014). Additionally, the SiO_2 coated shell chemistry is famous, which was convenience for conjugation of various biomolecules. Lu synthesized the hole of MIPs aiming at glycine molecules on the Fe_3O_4,

✉ Jianjun Shi
aust_jjshi@163.com

[1] School of Chemical Engineering, Anhui University of Science and Technology, 232001 Huainan, China

[2] Institute of Environment-friendly Materials and Occupational Health, Anhui University of Science and Technology, 241003 Wuhu, China

reducing amino acid of tryptophan static distribution coefficient (Lu et al. 2006). Dopamine readily self-polymerizes under alkaline conditions, forming a heterogeneous polymer coating on a wide variety of materials (Mao et al. 2012). PDA is a nontoxic biomolecular material bearing multifunctional amino and catechol groups, which make it appropriate for imprinting target objects. Inspired by this breakthrough, several studies on the preparation of MMIP nanoparticles by polymerizing DA have been reported (Yao et al. 2013; Deng et al. 2005). ECL sensors based on the QDs/potassium peroxydisulfate ($K_2S_2O_8$) system are common to use. Peng reported a water-soluble tungsten oxide QDs-based supersensitive ECL sensor platform with $K_2S_2O_8$ as the core reactant, which they used to detect dopamine (DA) released by P12 cells (Peng et al. 2019).

In this work, we present an ECL sensor based on core-shell magnetic particles and doped with QDs on a polydopamine (PDA)-based MIP, Fe_3O_4@SiO_2 was regard as an immobilization matrix to load MIP and QDs, imprinted QDs exhibiting strong ECL properties to determine trace BPA in the environment.

Materials and Methods

$FeCl_3$, ethylene glycol, NaAc, PEG, TEOS, 3-Amino-propyl-triethoxy-silane (APTES), Na_2HPO_4, NaH_2PO_4were supplied by Sinopharm Chemical Reagent Co., Ltd. BPA, DA, and Tris-HCl were purchased from Sigma-Aldrich. L-Cysteine and $CdCl_2$·$2.5H_2O$ were obtained from Fuchen Chemical Reagents Plant. Se and $NaBH_4$ was provided by Kermel Chemical Reagents Co., Ltd.

All chemicals used were of analytical grade and were used without further purification. Deionized water was used in all experiments.

The standard solution was used for BPA detection at the concentrations range from 10^{-8} mol L^{-1} to 10^{-3} mol L^{-1}. In selectivity testing, the concentration of potential interfering species (p-chlorophenol, p-phenylenediamine, phenol, p-aminophenol, p-nitrophenol) were 0.1 mmol L^{-1}.

Electrochemical measurements were performed with a CHI660D electrochemical workstation. The ECL emission was detected by means of an MPI-ECL analyzer at room temperature. FTIR spectra were recorded on an FTIR-850 spectrometer. UV/vis is absorption spectra were acquired with a UV-2550 spectrophotometer. Photoluminescence spectra were obtained on an F-4600 spectrophotometer. The sizes and morphologies of the MMIP particles were observed by means of a JEM-2100 F TEM.

The water samples were taken from the campus of Huainan, Anhui University of Science and Technology. Before testing, all water samples were filtered with a 0.5 μm filter membrane, and the filtrate was collected for use. 1 mL water sample solution was added into an electrolytic cell containing 9 mL 0.1 mol/L pH 7.0 PBS. The assembled sensor was placed in and the ECL technology was used to detect bisphenol A.

CdSe QDs were synthesized by a modification of a reported procedure (Jie et al. 2016). Briefly, L-cysteine and $CdCl_2$·$2.5H_2O$ (molar ratio 3) were dissolved in 150 mL of H_2O successively. Then, pH was adjusted to 10 with 1 mol·L^{-1} NaOH solution. Meanwhile, Se and $NaBH_4$ (molar ratio 1.5) were dissolved in 10 mL of water. The mixture was then heated at 40ºC for 30 min. The mixture was heated under reflux and maintained at 90ºC for 60 min. All experiments were conducted under conditions of nitrogen purging and magnetic stirring. The CdSe QDs were separated by precipitation from ethanol and centrifugation.

Fe_3O_4 nanoparticles were prepared according to previous method (Deng et al. 2005) with minor modifications. $FeCl_3$·$6H_2O$ (1.35 g) was dissolved in ethylene glycol (40 mL) to form a clear solution, followed by the addition of NaAc (3.6 g) and polyethylene glycol (1.0 g). The mixture was stirred vigorously for 30 min and then sealed in a Teflon-lined stainless-steel autoclave. The autoclave was heated to and maintained at 200°C for 8 h, and allowed to cool to room temperature. The black products were washed several times with ethanol and dried at 60°C for 6 h. In the next step, Fe_3O_4@SiO_2 nanoparticles (250 mg) were modified by dispersing them in anhydrous methanol (50 mL) containing APTES (5 mL) and allowing the derivatization to proceed for 24 h at room temperature.

Fe_3O_4@SiO_2-NH_2 nanoparticles (100 mg) and BPA (20 mg) were added to 10 mmol·L^{-1} pH 8.0 Tris buffer (20 mL) then stirred for 2 h at room temperature until a homogeneous suspension was obtained. CdSe QDs solution (20 mL) and DA (20 mg) were then added, and reaction was allowed to proceed for 3 h at room temperature. After polymerization, the template molecule (BPA) was leached out by using methanol/acetic acid (9:1, v/v) as an eluent, and the eluent was replaced every 30 min. BPA in the eluent was determined by UV/vis spectrophotometry (420 ~ 480nm). After complete removal of the BPA, the product (MMIP) was dried at 40ºC under vacuum. Similarly, magnetic non-molecularly imprinted polymer (MNIP) was prepared under the same conditions as described above, but with omission of the analyte.

An aliquot (5 μL) of the MMIP composite (or other product) solution was dropped on the surface of the electrode. The ECL tests, including the detection of BPA, were performed in 0.1 mol L^{-1} PBS (pH 7.4) containing 0.1 mol L^{-1} $K_2S_2O_8$ and 0.1 mol L^{-1} KCl, with CV scanning between 0 V and − 1.6 V at 100 mV s^{-1}. All experiments were performed at room temperature (25 ± 1ºC). Scheme 1 outlines the fabrication procedure of the ECL sensor based on an MMIP. First, the CdSe QDs were coated with L-cysteine

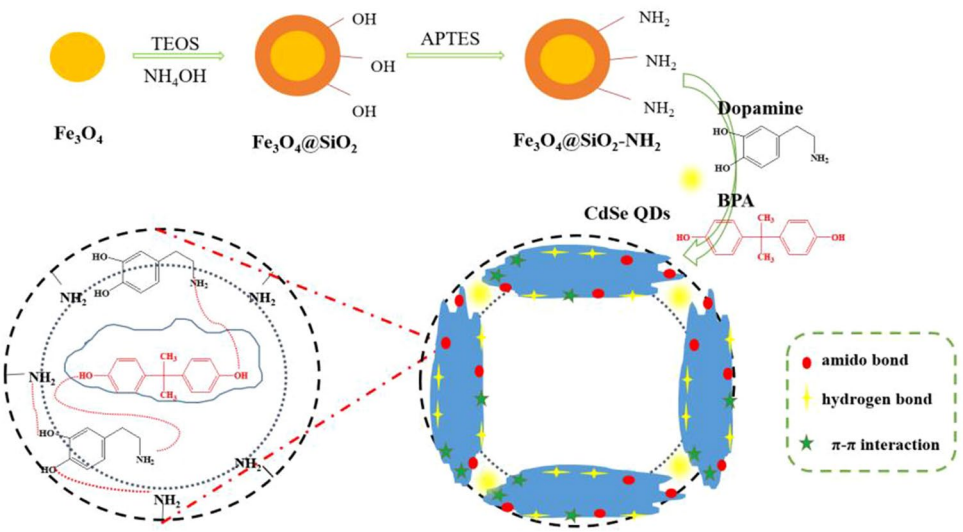

Scheme 1 Synthesis route of magnetic imprinted Fe_3O_4@SiO_2-MIP nanoparticles

through electrostatic interactions between Se and –SH. The -NH_2 and -COOH groups of L-cysteine anchored on the surface of the QDs participated in the polymerization process furnishing the MIP. The L-cysteine-modified CdSe QDs were doped in the core-shell magnetic material and reacted with DA through intermolecular forces under alkaline conditions; the BPA interacted with the DA through hydrogen-bonding.

Result and Discussions

Figure 1A and B shows TEM and HRTEM images of the synthesized magnetic nanoparticles. Evidently, the core with dark contrast represented a spherical Fe_3O_4 nanoparticle of size about 300 nm, the inner layer with medium contrast represented the SiO_2 shell with a thickness of 50 nm, and the outer discontinuous layer with light contrast represented the MIP shell with average thickness 12 nm. In addition, in the MIP layer, a lattice fringe of 0.325 nm could be clearly discerned, corresponding to the crystalline interplanar spacing of CdSe QDs. Thus, doping with CdSe QDs had been successfully accomplished. In Fig. 1C, the peaks of curve a located at 440 cm^{-1} and 579 cm^{-1} could be attributed to the vibrational bands of Fe-O and Fe-OH bonds (Lu et al. 2006), and that at 3414 cm^{-1} could be attributed to the magnetite structure in the lattice of Fe_3O_4. In curve b, the covalent bond between the silane and magnetite surface gave rise to the band at 1102 cm^{-1}, which was characteristic of Si-O bonds, and the -OH group gave rise to peaks at around 1638 cm^{-1} and 3414 cm^{-1} (Mao et al. 2012). The results supported the immobilization of SiO_2 on the surface of the Fe_3O_4@SiO_2 core-shell structure. Curve c shows the spectrum of Fe_3O_4@SiO_2-NH_2. The peaks at 960 cm^{-1} and 810 cm^{-1} were indicative of a disubstituted benzene, and that at 460 cm^{-1} corresponded to Si-C bonding.

VSM images are illustrated in Fig. 1D. It was obvious that there was no hysteresis; both the remanence and coercivity were zero, indicating that the samples exhibited superparamagnetic behavior (Xu et al. 2006). The saturation magnetization values obtained at room temperature were 70.5 emu g^{-1}, 35.3 emu g^{-1}, and 1.9 emu g^{-1} for Fe_3O_4, Fe_3O_4@SiO_2, and Fe_3O_4@SiO_2-MIPs, respectively. The decrease in magnetization could be attributed to the SiO_2 and MIP layer shielding the magnetite effectively, since the extent of dipolar coupling is related to the distance between the particles and this in turn depends on the thickness of the shell (Liu et al. 2009). However, the saturation magnetization value of Fe_3O_4@SiO_2-MIPs were high enough for separation from the sample solution.

Figure 2 A shows the fluorescence and UV/vis absorption spectra of the CdSe QDs in aqueous solution. The fluorescence emission peak at 554 nm (λ_{ex} = 370 nm) and the absorption peak ranging from 420 nm to 480 nm reflected the consequence of quantum confinement. The inset shows a vial of CdSe QDs illuminated at 370 nm, displaying a blue aura. At a certain concentration of CdSe QDs, the ECL intensity could reach about 4500 a.u., as shown in Fig. 2B, as reported previously (Jie et al. 2016). The possible reason for the ECL detection may be described as follows: $CdSe^-$ generated from the CdSe QDs combined with the strong oxidant $SO_4^{\bullet-}$ to produce an excited-state species $CdSe^*$, which emits light in aqueous solution. The inset in Fig. 2B displays the CV of the CdSe QDs, which featured a cathodic peak at −1.0 V and an anodic peak at −0.7 V. These results suggested a similar mechanism to that reported previously (Ke et al. 2015; Jiao et al. 2017). The peak at −1.0 V could be attributed to electrochemical reduction of CdSe QDs on the electrode, which generated nanocrystalline radicals ($CdSe^-$), and the peak at −0.7 V could be ascribed to the reduction of $S_2O_8^{2-}$ to sulfate anion radicals ($SO_4^{\bullet-}$). Based

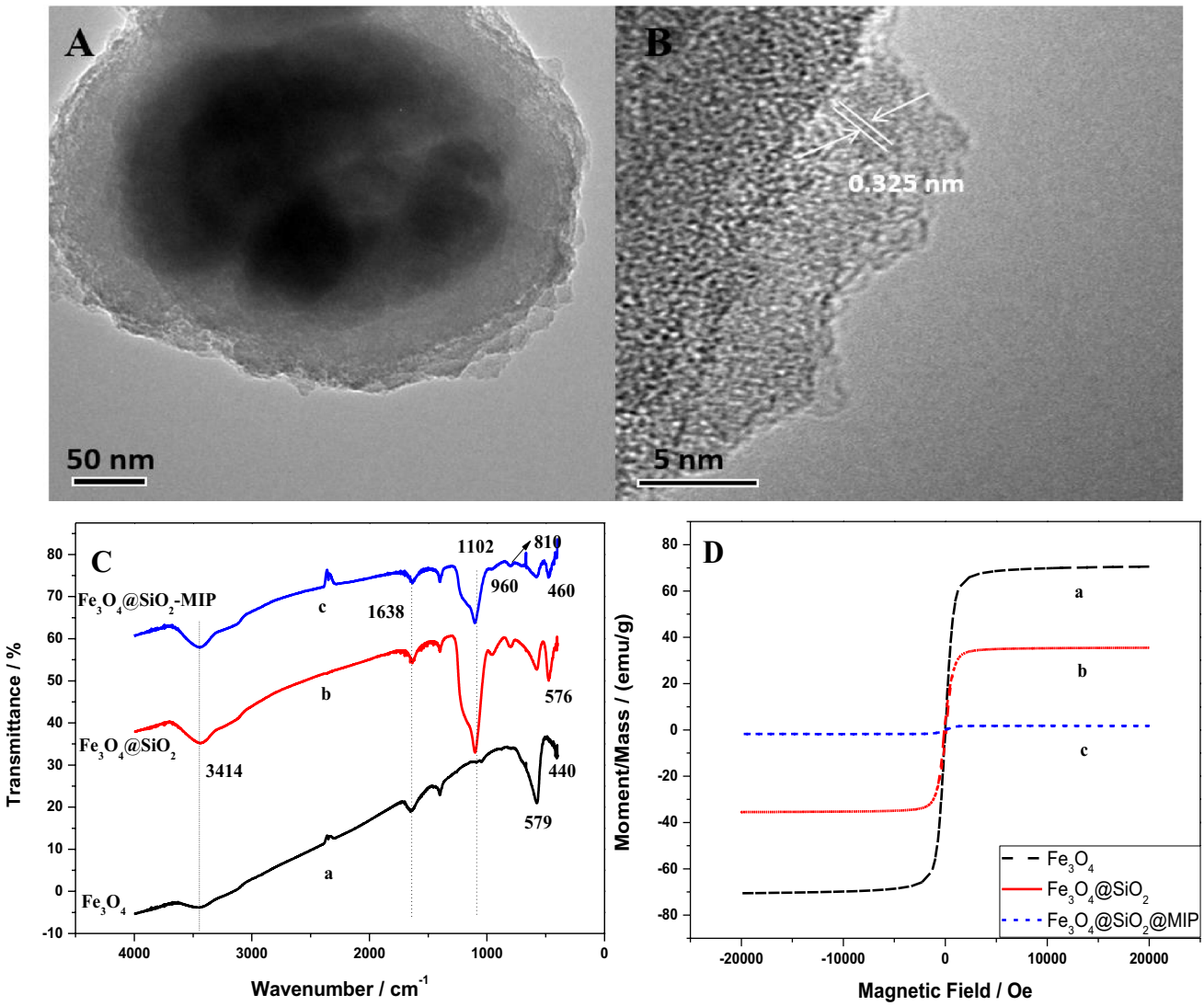

Fig. 1 **A** TEM and **B** HRTEM of Fe_3O_4@SiO_2-MIP **C** FT-IR spectrum **D** VSM curves (a) Fe_3O_4, (b) Fe_3O_4@SiO_2, and (c) Fe_3O_4@SiO_2-MIP nanoparticles

on the experimental results and ECL quenching mechanisms reported previously (Liu et al. 2009; Ke et al. 2015; Jiao et al. 2017), a mechanism for the inhibition of ECL in the $K_2S_2O_8$/QDs/BPA system is proposed, as shown in Fig. 2D.

In Fig. 2C, before removal of the template molecules, the ECL intensity of the Fe_3O_4@SiO_2-MIP(QDs) (about 350 a.u.) (curve a) was far lower than that of the Fe_3O_4@SiO_2-NIP(QDs) (about 2200 a.u.) (curve c). After the removal of template molecule, the ECL intensity of the Fe_3O_4@SiO_2-MIP(QDs) (about 1900 a.u.) in curve b was increased. This result indicated that the template molecule (BPA) was cleanly removed from the composite and that it had a quenching effect of BPA on the ECL (Zhao et al. 2020).

Figure 3A displays the ECL intensity of the sensor after adding BPA solutions of different concentrations to the MIP system under the optimized experimental conditions. It was obvious that the ECL intensity of the sensor gradually decreased with increasing BPA concentration and then remained stable for a certain time. Each point in Fig. 3B is an average value of three repeated measurements, and the error bar is the standard deviation. The linear equation shown in Fig. 3B is $y = -336.30x - 700.08$, with $R_2 = 0.9728$. The ECL peak intensity was linear with the BPA concentration from 10^{-4} to 10^{-9} mol L^{-1} with a detection limit of 3.4×10^{-10} mol L^{-1} (S/N = 3), indicating that this sensor exhibited remarkable reliability. Figure 3C shows the ECL intensity responses of solutions containing 0.1 mmol L^{-1} BPA and the potential interfering species. Comparing the ECL intensity responses, those with the analogues were all three times higher than that with BPA,

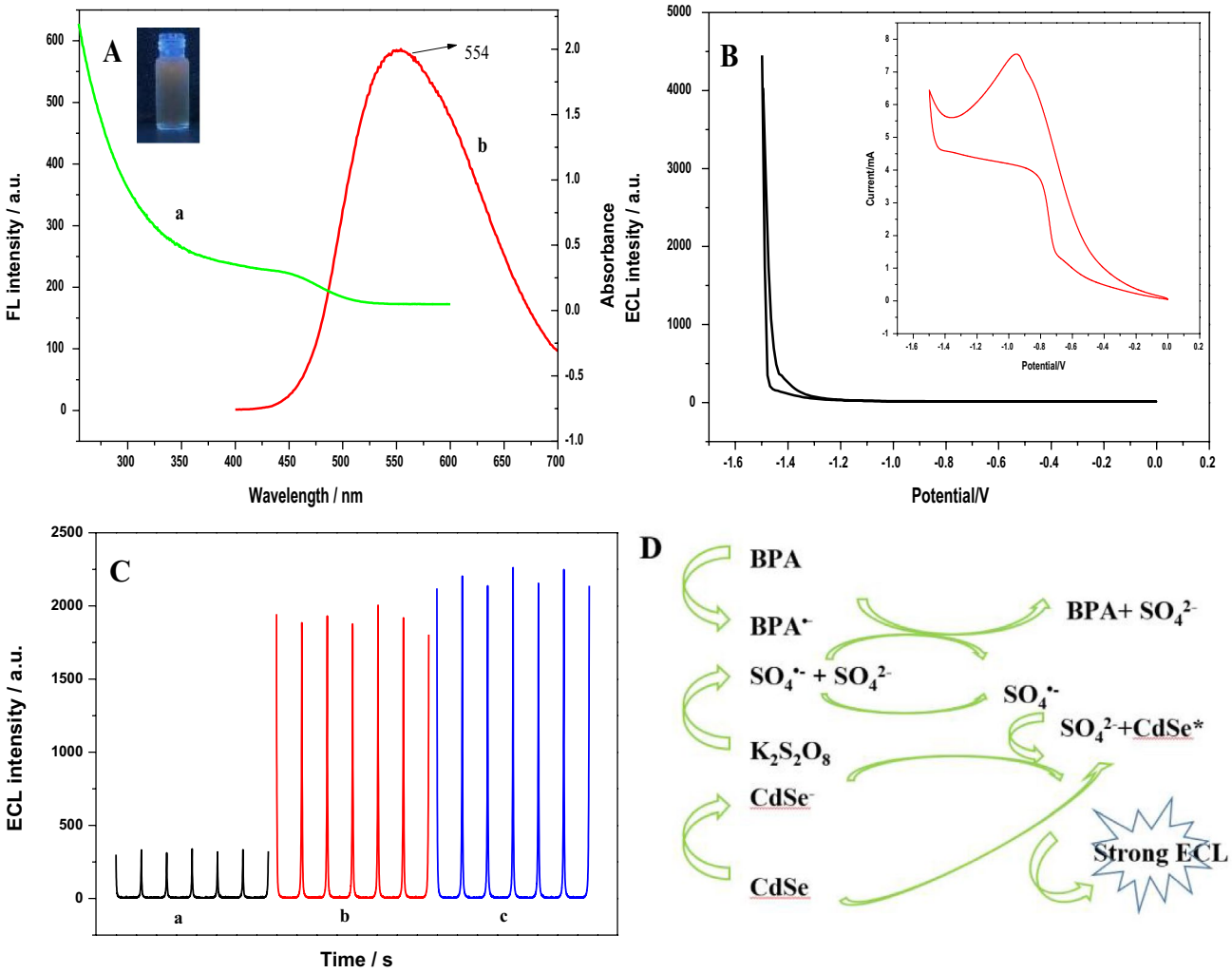

Fig. 2 **A** UV-vis absorption spectra and Fluorescence spectra of CdSe QDs; **B** ECL intensity-potential of CdSe QDs (insert: CV); **C** ECL intensity of doping QDs form (a) MIP (before wash); (b) MIP (after wash); (c) NIP; **D** Mechanism for the ECL $K_2S_2O_8$/QDs/BPA system

indicating good selectivity. It was observed that phenol had a slight quenching effect. This could be attributed to the small size of phenol compared to BPA, which allowed it to easily penetrate into the imprinted cavities in the polymer backbone. The above results revealed that the MMIP sensor exhibited high recognition selectivity towards BPA, with almost no interference from the analogues.

The standard recovery method was adopted to simulate the detection of BPA in actual water samples. The samples were then spiked with three concentration levels of a standard solution of BPA. The BPA in the different water samples was determined with the MMIP sensor, and the results are listed in Table 1. The recoveries of BPA achieved were in the range 96%–107%. Thus, the MMIP sensor proved to be highly sensitive and gave almost quantitative recoveries. These results clearly indicated that the sensing system-based MIP presented here was valid for real sample analysis and was not hampered by matrix effects.

The comparison of the proposed BPA sensor with previously reported was shown in Table 2. It can be seen that the sensor has a low detection limit and a wide detection range.

Conclusions

A new electrochemical luminescent sensor based on a magnetic core–shell structure has been constructed and used for the detection of bisphenol A. Hydrothermal and self-polymerization methods have been applied to prepare Fe_3O_4 and Fe_3O_4@SiO_2-MIP magnetic nanoparticles, respectively, with both products being spherical in shape with uniform particle size. Coating the Fe_3O_4 surface with a silica layer improved the stability and

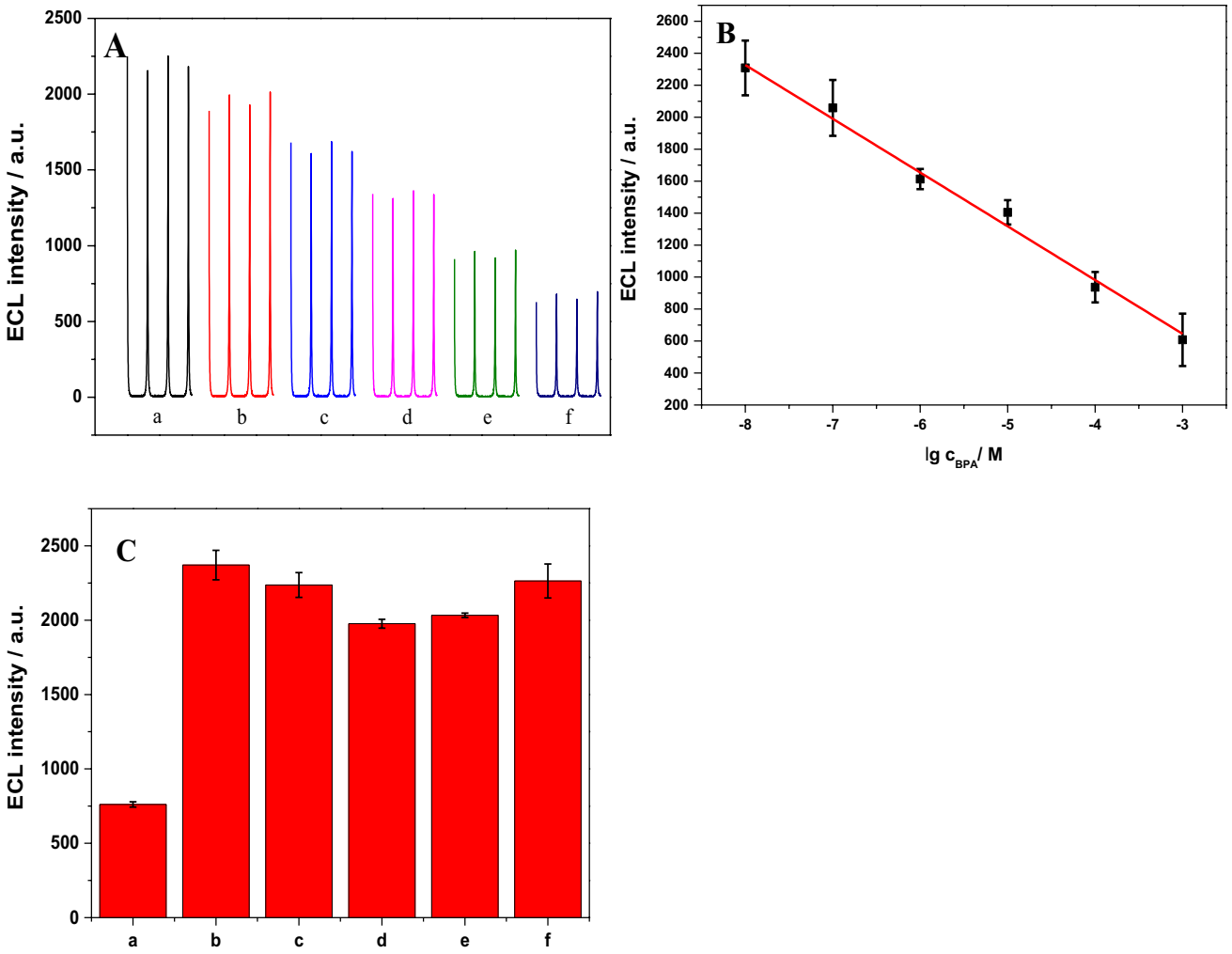

Fig. 3 **A** ECL intensity of the sensor for BPA detection at different concentrations a-f, 10^{-8} mol L^{-1} to 10^{-3} mol L **B** Calibration curve for BPA detection; **C** ECL intensity of MIPs. a–f correspond to BPA, p-chlorophenol, p-phenylenediamine, phenol, p-aminophenol, p-nitrophenol (0.1 mmol L^{-1})

Table 1 Determination of BPA in the nature water samples ($n=5$)

Samples [a]	Added (nmol L^{-1})	Founded (nmol L^{-1})	RSD (%)	Recovery (%)
A	0	3.2	4.5	96
	10	12.8	5.7	
B	0	7.2	2.9	107
	10	17.9	4.6	
C	0	5.5	6.7	106
	10	16.1	5.4	

[a] Water samples were collected from rainwater (A) and local river (B), C is distilled water for blank marking recovery

ease of functionalization. Although the diameter of the Fe_3O_4@SiO_2-MIP nanoparticles was greater than that of the unmodified Fe_3O_4 nanoparticles, they maintained strong superparamagnetic and magnetic field induction performances, and could be easily separated. In addition, by doping with quantum dots through dopamine self-polymerization, the system was endowed with good electrochemical luminescence properties and could be used for ECL testing. Based on the interaction between bisphenol A, the quantum dots, and co-reagents in the detection process, electron conduction at the electrode surface produced optical signals. The detectable concentration range of bisphenol A was 1×10^{-9} to 1×10^{-4} mol L^{-1}, and the limit of detection was 3.4×10^{-10} mol L^{-1}. The developed sensor had high sensitivity, convenient operation, good stability, and high reproducibility. It thus provides an effective new method for the detection of environmental contaminants in industrial wastewater and river water, and shows significant application prospects in this field. Besides, the establishment of soil standards for bisphenol A for soil ecosystem protection would also be meaningful.

Table 2 Comparison of the proposed sensor with previously reported

Materials	Detection range (mol L^{-1})	Limit (mol L^{-1})	References
GO[a]/APTES–MIP	2.0×10^{-7}–2.0×10^{-5}	3.0×10^{-9}	Dadkhah et al. (2016)
MWCNT[b]–MAM[c]	1.0×10^{-8}–4.08×10^{-5}	5.0×10^{-9}	Li et al. (2012)
PAMAM[d]–Fe_3O_4	1.0×10^{-8}–3.07×10^{-6}	5.0×10^{-9}	Yin et al. (2011)
Fe_3O_4@SiO_2-MIP	1.0×10^{-9}–1.0×10^{-4}	3.4×10^{-10}	This work

[a] Graphene oxide. [b] Multiwall carbon nanotube. [c] Melamine. [d] Polyamidoamine dendrimer

Acknowledgements We greatly appreciate the support of the National Natural Science Foundation of China (21505001), the Major Programs of Science and Technology of Anhui Province (201903a06020003).

References

Dadkhah S, Ziaei E, Mehdinia A, Baradaran Kayyal T, Jabbari AJ (2016) A glassy carbon electrode modified with amino-functionalized graphene oxide and molecularly imprinted polymer for electrochemical sensing of bisphenol A. Microchim Acta 183(6):1933–1941

Deng H, Li X, Peng Q, Wang X, Chen J, Li YD (2005) Monodisperse magnetic single-crystal ferrite microspheres. Angew Chem Int Ed 44:2782–2785

Fernandez MAM, Andre LC, Cardeal ZL (2017) Hollow fiber liquid-phase microextraction-gas chromatography-mass spectrometry method to analyze bisphenol A and other plasticizer metabolites. J Chromatogr A 1481:31–36

Freitas JM, Wachter N, Rocha-Filho RC (2020) Determination of bisphenol S, simultaneously to bisphenol A in different water matrices or solely in electrolyzed solutions, using a cathodically pretreated boron-doped diamond electrode. Talanta 217:121041

Jiao M, Jie GF, Tan L, Niu SY (2017) AgNPs-3D nanostructure enhanced electrochemiluminescence of CdSe quantum dot coupled with strand displacement amplification for sensitive biosensing of DNA. Anal Chim Acta 983:166–172

Jie G, Chen K, Wang X, Lu ZK (2016) Dual-stabilizer-capped CdSe quantum dots for "Off–On" electrochemiluminescence biosensing of thrombin by target-triggered multiple amplification. RSC Adv 6(3):2065–2071

Ke R, Zhang XM, Wang L, Zhang CY, Zhang S, Mao CJ, Niu HL, Song J, Jin BK, Tian YP (2015) Electrochemiluminescence sensor based on Graphene Oxide/Polypyrrole/CdSe nanocomposites. J Alloys Compd 622:1027–1032

Li YG, Gao Y, Cao Y, Li H (2012) Electrochemical sensor for bisphenol A determination based on MWCNT/melamine complex modified GCE. Sensor Actu B 171:726–733

Li ZH, Zhang WQ, Shan BQ (2019) The effects of urbanization and rainfall on the distribution of, and risks from, phenolic environmental estrogens in river sediment. Environ Pollut 250:1010–1018

Liu JY, Martin JW (2017) Prolonged exposure to bisphenol A from single dermal contact events. Environ Sci Technol 51(17):9940–9949

Liu Y, Li HF, Lin JM (2009) Magnetic solid-phase extraction based on octadecyl functionalization of monodisperse magnetic ferrite microspheres for the determination of polycyclic aromatic hydrocarbons in aqueous samples coupled with gas chromatography-mass spectrometry. Talanta 77(3):1037–1042

Liu SF, Zhang X, Yu YM, Zou GZ (2014) A Monochromatic electrochemiluminescence sensing strategy for dopamine with dual-stabilizers-capped CdSe quantum dots as emitters. Anal Chem 86(5):2784–2788

Lu SL, Cheng GX, Zhang HG, Pang XG (2006) Preparation and characteristics of Tryptophan-imprinted Fe3O4/P(TRIM) composite microspheres with magnetic susceptibility by inverse emulsion–suspension polymerization. J Appl Polym Sci 99(6):3241–3250

Mao Y, Bao Y, Han D, Li F, Niu L (2012) Efficient one-pot synthesis of molecularly imprinted silica nanospheres embedded carbon dots for fluorescent dopamine optosensing. Biosens Bioelectron 38(1):55–60

Peng CF, Pan N, Xie ZJ, Liu L, Xiang J, Liu C (2016) Determination of bisphenol A by a gold nanoflower enhanced enzyme-linked immunosorbent assay. Anal Lett 49(10):1492–1501

Peng H, Liu P, Wu W, Chen W, Meng X, Lin X, Liu A (2019) Facile electrochemiluminescence sensing platform based on water-soluble tungsten oxide quantum dots for ultrasensitive detection of dopamine released by cells. Anal Chim Acta 1065:21–28

Wang X, Lu X, Wu L, Chen J (2015) 3D metal-organic framework as highly efficient biosensing platform for ultrasensitive and rapid detection of bisphenol A. Biosens Bioelectron 65:295–301

Wang S, Liu F, Wu W, Hu Y, Liao R, Chen G, Wang J, Li J (2018) Migration and health risks of nonylphenol and bisphenol a in soil-winter wheat systems with long-term reclaimed water irrigation. Ecotox Environ Safe 158:28–36

Watabe Y, Kondo T, Imai H, Morita M, Tanaka N, Haginaka J, Hosoya K (2004) Improved detectability with a polymer-based trapping device in rapid HPLC analysis for ultra-low levels of bisphenol A (BPA) in environmental samples. Anal Sci 20(1):133–137

Xu XQ, Deng CH, Gao MX, Yu WJ, Yang PY, Zhang XM (2006) Synthesis of magnetic microspheres with immobilized metal Ions for enrichment and direct determination of phosphopeptides by matrix-assisted laser desorption ionization mass spectrometry. Adv Mater 18(24):3289–3293

Yao GH, Liang RP, Huang CF, Wang Y, Qiu JD (2013) A surface plasmon resonance sensor based on magnetic molecularly imprinted polymers amplification for pesticide recognition. Anal Chem 85(24):11944–11951

Yin H, Cui L, Chen Q, Shi W, Ai S, Zhu L, Lu LJ (2011) Amperometric determination of bisphenol A in milk using PAMAM–Fe_3O_4 modified glassy carbon electrode. Food Chem 125(3):1097–1103

Zhao WR, Xu YH, Kang TF, Zhang X, Liu H, Ming AJ, Cheng SY, Wei F (2020) Sandwich magnetically imprinted immunosensor for electrochemiluminescence ultrasensing diethylstilbestrol based on enhanced luminescence of Ru@SiO2 by CdTe@ZnS quantum dots. Biosens Bioelectron 155:112102